

HIGH COLUMN DENSITIES AND LOW EXTINCTIONS OF γ -RAY BURSTS:
EVIDENCE FOR HYPERNOVAE AND DUST DESTRUCTIONTITUS J. GALAMA^{1,2} AND RALPH A.M.J. WIJERS³*Draft version October 24, 2018*

ABSTRACT

We analyze a complete sample of γ -ray burst afterglows, and find X-ray evidence for high column densities of gas around them. The column densities are in the range $10^{22} - 10^{23} \text{ cm}^{-2}$, which is right around the average column density of Galactic giant molecular clouds. We also estimate the cloud sizes to be 10–30 pc, implying masses $\gtrsim 10^5 M_{\odot}$. This strongly suggests that γ -ray bursts lie within star forming regions, and therefore argues against neutron star mergers and for collapses of massive stars as their sources. The optical extinctions, however, are 10–100 times smaller than expected from the high column densities. This confirms theoretical findings that the early hard radiation from γ -ray bursts and their afterglows can destroy the dust in their environment, thus carving a path for the afterglow light out of the molecular cloud. Because of the self-created low extinction and location in star-forming regions, we expect γ -ray bursts to provide a relatively unbiased sample of high-redshift star formation. Thus they may help resolve what is the typical environment of high-redshift star formation.

Subject headings: gamma rays: bursts — cosmology — extinction — stars: formation

1. INTRODUCTION

γ -ray bursts emit up to 10^{53} ergs in gamma rays and X rays in a few seconds, followed by an ‘afterglow’ of X-ray (Costa et al. 1997), optical (Van Paradijs et al. 1997) and radio (Frail et al. 1997) emission that generally lasts days to months (Van Paradijs, Kouveliotou, & Wijers 2000). The arcsecond localizations of γ -ray bursts by the detection of these counterparts have made it possible to study the environments in which γ -ray bursts arise. This has provided a number of indications of their association with massive stars and star formation. First, most γ -ray bursts lie within the region of UV emission from massive stars in their host galaxy. Second, the energies of γ -ray bursts are comparable to those of supernovae, further suggesting the deep gravitational collapse of a few solar masses as the source of energy for γ -ray bursts. Candidates satisfying these requirements include exploding very massive stars, also termed hypernovae or collapsars (Woosley 1993, Paczyński 1998), mergers of two neutron stars (Eichler et al. 1989) and the merger of a neutron star and a black hole (Mochkovitch et al. 1993). Mergers may be inconsistent with the small offsets between γ -ray bursts and their hosts (Bloom et al. 1999b, Bulik et al. 1999). Further evidence for the relation between γ -ray bursts and star formation has been provided by the fact that the brightness distribution of γ -ray bursts agrees well with models in which the γ -ray burst rate tracks the star formation rate over the past 15 billion years of cosmic history (Totani 1997, Wijers et al. 1998, Kommers et al. 2000). The most direct evidence relating γ -ray bursts to a specific type of progenitor has been the discovery of supernova 1998bw in the error box of GRB 980425 (Galama et al. 1998b) and the detection of supernova-like light curves underneath two afterglows, GRB 980326 (Bloom et al. 1999a) and GRB 970228 (Reichart 1999, Galama

et al. 2000). Despite their unusually high luminosity, these supernovae would often go unnoticed due to the much brighter γ -ray burst afterglow; therefore, we do not know whether most γ -ray bursts are associated with supernovae or just some of them. Also, the fact that GRB 980425 was very nearby and subluminous in gamma rays by a factor 10^4 makes it hard to extrapolate its supernova association to normal γ -ray bursts without additional considerations.

To elucidate the γ -ray burst-supernova association further, we examine optical and X-ray extinctions of γ -ray burst afterglows (Sect. 2). Then we discuss the evidence these extinctions provide that the majority of long γ -ray bursts occur in molecular clouds, with dust destruction explaining the unusually low extinctions (Sect. 3). We thus infer that neutron star and black-hole mergers are no longer plausible γ -ray burst progenitors, and briefly mention some further implications of our results (Sect. 4).

2. EXTINCTION OF γ -RAY BURST AFTERGLOWS2.1. *Optical extinction*

A paradox in associating most γ -ray bursts with exploding very massive stars is that one expects the majority of these to lie amidst highly absorbing molecular clouds. The lack of high restframe visual extinction has therefore led to considerable skepticism about the γ -ray burst-supernova connection. Here we reinvestigate the extinction for γ -ray bursts in a systematic way, by fitting an extinction model to all afterglows for which the required X-ray and optical data exist. The model function is

$$F_{\nu} = F_{V0} [\nu/\nu_V]^{-\beta} \exp[-A_{Vr}(1+z)\nu/\nu_V], \quad (1)$$

where ν_V and F_{V0} are the observer-frame V band central frequency and extinction-corrected V band flux, respectively, and A_{Vr} is the rest frame visual extinction; the extinction term is applied only to optical and infrared data.

¹Division of Physics, Mathematics and Astronomy, California Institute of Technology, MS 105-24, Pasadena, CA 91125; tjg@astro.caltech.edu

The results of the fits are given in table 1. Note the low optical extinctions. (Some fitted A_{V_T} are negative, as expected from a fit procedure if the values are less than the fit errors; we did not force $A_V > 0$.) We have used the simplest possible extinction law here, $A_\nu \propto \nu$. In metal-rich environments, the extinction can have features, such as the 2200Å ‘bump’. We see no significant detection of this bump in any afterglow, despite its easy observability at redshifts 1–2, and therefore neglect it.

The prompt and afterglow X rays are not significantly attenuated, and there is only one γ -ray burst in which the search for an optical afterglow resulted in upper limits well below the expected optical flux (GRB 970828; Groot et al. 1998⁴.) Most optical non-detections are adequately explained by adverse observing conditions, and consistent with the presence of a normal afterglow. Hence there is no evidence from non-detections for a significant population of highly extinguished γ -ray bursts, or for significant skewing of the extinction distribution due to the selection effect that γ -ray bursts with higher extinction are simply not found.

In the above analysis, we have assumed that the intrinsic spectrum of the afterglow is a pure power law. The theory of afterglows allows a so-called ‘cooling break’ in the spectrum between X rays and optical, where the power-law slope steepens by 1/2. A comparison of the mean optical-to-X-ray slope, β_{OX} , and the X-ray spectral slope, β_X , shows that they are indeed different, indicating that such a break may be present: $\langle \beta_X - \beta_{OX} \rangle = 0.31 \pm 0.05$. Therefore we redo our fits with an extra break. The fit function is

$$F_\nu = F_{V0}[\nu/\nu_V]^{-(\beta+1/2)} \exp[-A_{V_T}(1+z)\nu/\nu_V] \times \left(\frac{[\nu(1+z)/\nu_c]^{-n/2} + 1}{[\nu_V(1+z)/\nu_c]^{-n/2} + 1} \right)^{-1/n}. \quad (2)$$

The index n controls the sharpness of the break. We use $n = 2$, which provides a smooth transition over 2 dex in frequency, and find little change in the fits if we vary the width in the range 1–3 dex. The extra datum needed to constrain this fit is β_X . To treat this uniformly with the other data, we add an artificial data point with ten times greater frequency than the first X-ray point, and give it a value and error so that a fit to the two X-ray points gives the correct values and errors of the X-ray flux and spectral slope. The results of the new fits are also given in table 1, showing hardly any change in the extinctions.

2.2. X-ray absorption

Our results confirm in a more rigorous way the casual impression of low optical extinction in γ -ray bursts and therefore seem to contradict the notion of exploding massive stars being the progenitors of γ -ray bursts. However, the hydrogen column densities towards the γ -ray bursts reveal startlingly contrasting evidence. In table 1 we collect from the literature values of the hydrogen column density towards γ -ray bursts as derived from soft X-ray absorption. To obtain these values, we subtracted the Galactic foreground column (Dickey & Lockman 1990) from the total measured value. Then we accounted for the fact that

$\tau_X \propto E^{-2.6}$ (Morrison & McCammon 1983), which implies that we have to multiply the foreground-subtracted column by $(1+z)^{2.6}$ for a source at redshift z , to get the true column density in the rest frame of the γ -ray burst. (Note that while in principle the photoelectric absorption has richer structure due to absorption edges of individual atomic species, the presently available spectral resolution and S/N does not allow this to be discerned.) This is a large correction, ranging from 4 to 50 among the sample, and the resulting restframe hydrogen column densities are in the range $10^{21.5} - 10^{23.3} \text{ cm}^{-2}$. To emphasize the contrast between the optical and X-ray results, we show in Figure 1 the correlation between optical and X-ray extinction. The solid curve indicates the relation between A_V and N_H for the Milky Way (Predehl & Schmitt 1995), so we see that the observed visual extinctions are 10–100 times smaller than expected for the observed X-ray absorption.

Both types of extinction are due to heavy elements, so metallicity differences cannot change the ratio. However, the optical/UV extinction is due to dust grains, whereas the X-ray extinction is due to K- and L-shell electrons of intermediate-mass elements (mostly C and O) and therefore does not depend on whether the atoms are in a gas or a solid. The X-ray extinction is therefore a better measure of the total column density. However, converting the X-ray absorption to a hydrogen column density, as is customary, *does* depend on metallicity. Since the high-redshift regions we are probing may have lower metallicities, the true column densities can only be larger than those we have derived. (Since the regions are very actively star forming, their metallicity may not be much less than in the Milky Way, though.)

3. IMPLICATIONS FOR γ -RAY BURST ENVIRONMENTS

The values of the X-ray column densities are very high, and typical of the column densities through giant molecular clouds (Fig. 1; Solomon et al. 1987). This strongly suggests that most γ -ray bursts are located in molecular clouds. We now attempt to constrain the size of the clouds, and thereby their mass.

First, the surprisingly low extinctions may be explained by recently proposed dust destruction: dust is sensitive to the UV and X-ray radiation from the γ -ray burst and its afterglow. UV and X-ray light heats the grains, and out to about 20 pc can evaporate them (Waxman & Draine 2000, Fruchter et al. 2000). Waxman and Draine find that a prompt flash like that seen only in GRB 990123 is needed to muster enough UV light; however, Fruchter et al. show that the X-ray flux is at least as efficient in heating the grains. Since these come mostly from the prompt burst emission, the uncertain UV flashes are not needed in their model. They find that average γ -ray bursts can evaporate all dust out to 20 pc. Beyond this, dust may be shattered by strong grain charging. Since the effect of this on dust extinction properties is unclear, we shall not consider it here. From our low optical extinctions, we conclude that dust destruction must be taking place. This limits the bulk of the cloud to lie within about 20 pc of the γ -ray burst.

follows from the fact that the afterglow radius after a day is about 0.1 pc (e.g., Wijers & Galama 1999). This firmly excludes any remains of the exploded star as the source of X-ray or optical absorption. The size of the absorbing cloud can also be bounded from below using absorption lines of MgI in the spectra of many optical transients (e.g., Vreeswijk et al. 2000, Metzger et al. 1997). Afterglows tend to have strong MgI lines, especially relative to MgII, indicating they originate in denser regions than the normal diffuse ISM. We therefore suppose they originate in the same region that causes the large X-ray columns. The fact that this MgI is still visible after a day means it has not all been ionized away. MgI has an ionization energy of 7.84 eV, and photons above 13.6 eV are stopped by H very near the γ -ray burst. Averaging the ionization cross section over this energy range, weighted by the afterglow fluence spectrum, we find an optical depth to MgI ionizing photons of $0.7N_{\text{H}22.5}$ (assuming the solar value of $[\text{Mg}/\text{H}]$). This means that for most of the column density range, the optically thin limit is adequate for judging the survival of MgI at the edge of the cloud. Recombination times are much too long to play a role.

Integrating the γ -ray burst flux over time and over the same energy range, weighted by the energy-dependent cross section, we find that an average Mg atom would intercept $2.1 \times 10^4 E_{52}^{4/3} n^{1/2} \epsilon_{B,-2}^{5/6} \epsilon_{e,-1}^{4/3} (d/1 \text{ pc})^{-2}$ ionizing photons (for a typical afterglow with $\beta = 0.75$, where $\epsilon_B = 0.01\epsilon_{B,-2}$ and $\epsilon_e = 0.1\epsilon_{e,-1}$ are the equipartition fractions in the notation of Wijers & Galama 1999). Therefore, some of the Mg must be many parsecs from the γ -ray burst in order to survive. The Mg lines are usually rather saturated, so we can only get a lower limit to the MgI column density. For the case of GRB 990510 (Vreeswijk et al. 2000), this limit is $10^{13.3} \text{ cm}^{-2}$, which for normal Mg abundance is contained in less than 10^{21} cm^{-2} of total N_{H} , accounting for depletion. This is less than the total observed X-ray column, so only a fraction of Mg need remain neutral. To set a conservative lower limit, we shall tolerate 10 ionizations for the average Mg atom at the edge, implying survival of less than $e^{-10} = 5 \times 10^{-5}$ of Mg anywhere in the cloud. Then the lower limit to the cloud size becomes $45 E_{52}^{2/3} n^{1/4} \epsilon_{B,-2}^{5/12} \epsilon_{e,-1}^{2/3} \text{ pc}$. This is quite sensitive to burst parameters, and often above the upper limit from dust destruction. Therefore, Mg lines need not occur in every burst, and their presence should be correlated with burst strength.

Together, dust destruction and MgI survival constrain the size of the cloud to be tens of parsecs. The cloud therefore has a density of $500 N_{\text{H}22.5}/R_{20} \text{ cm}^{-3}$ and a mass of $4 \times 10^5 N_{\text{H}22.5} R_{20}^2 M_{\odot}$ (where $N_{\text{H}22.5} = N_{\text{H}}/10^{22.5} \text{ cm}^{-2}$ and $R_{20} = R/20 \text{ pc}$). These parameters are very much like those of giant molecular clouds (Solomon & Edmunds 1980, Solomon et al. 1987). We therefore consider our findings strong evidence that almost all (long) γ -ray bursts are associated with giant molecular clouds, and therefore with star-forming regions. This, in turn, speaks in favor of massive stars rather than compact-object mergers as the progenitors of γ -ray bursts.

Further predictions of the location of γ -ray bursts in molecular clouds are associated with absorption/scattering

frared may produce a reradiation echo with a thermal spectrum that peaks in restframe infrared on a time scale of several tens of days (Waxman & Draine 2000). (ii) Scattering of the afterglow's light by dust outside the dust-vacated region may produce a scattering echo on time scales of tens to hundreds of days (Esin & Blandford 2000). This echo has a spectrum similar to that of the afterglow. Each echo can emit 10^{41-42} erg/s . (iii) The far UV radiation will be absorbed by H_2 , causing a strong drop in the UV at 1650 Å and 1300 Å, and fluorescence will result in restframe UV emission on time scales of days to months (Draine 2000). (iv) If burst radiation is collimated, it is likely that the later, softer emission is less collimated, enabling us to see more afterglows than γ -ray bursts (e.g., Rhoads 1997). However, because dust is destroyed only along the collimated path of the initial hard radiation, such ' γ -ray burst-less afterglows' would not be visible in optical and near-IR from embedded sources. Only in far-IR, mm, and radio could the frequency of afterglows be significantly greater than that of γ -ray bursts.

Our findings may also have some indirect bearing on the issue of the cosmic star formation history, in the following sense: there has been much recent debate on the relative importance of UV and far-IR radiation in counting the star formation rate at high redshift (e.g., Madau et al. 1998, Barger et al. 1999). In both cases, one counts the location of massive, UV-producing stars, but in the far-IR case it is found/assumed that the majority of these are deeply shrouded in dust, concentrated in ultraluminous IR galaxies (ULIGs, e.g. Sanders & Mirabel 1996). Since γ -ray burst radiation escapes fairly well even from ULIGs, γ -ray burst locations might provide an unbiased sample of massive-star locations at redshifts 1–4. This means that a far-IR study of γ -ray burst host galaxies should help resolve the issue of what type of host, ULIGs or UV-emitting smaller galaxies, are the dominant source of massive-star production at these redshifts.

4. CONCLUSIONS

We have examined a complete sample of γ -ray burst afterglows, namely those with known redshift and X-ray column density, for which optical to X-ray data allow a determination of reddening. As a sample, they provide strong evidence for high X-ray column densities, without a single good exception. However, the individual measurements in a given source are very significant only for GRB 980703 and GRB 980329. Therefore, good X-ray spectra are required for more sources in order to confirm our findings and pin down the parameters of the clouds better. The size and origin of the absorbing matter are constrained by the low extinction, the blast wave size, and the survival of MgI. High-resolution measurements of the Mg absorption lines to better determine the location and column density of the Mg absorber are needed to strengthen the lower limits on cloud size and mass.

In short, we find high X-ray column densities and low optical extinctions for γ -ray burst afterglows, from which we infer that (i) Most γ -ray bursts are embedded in large molecular clouds. (ii) γ -ray bursts are therefore likely produced by dying massive stars, and not by mergers of neutron stars and/or black holes. (iii) The low optical extinc-

for the optical afterglow to escape even large clouds. (iv) γ -ray burst host studies may help identify the dominant sources of high-redshift star formation.

We are grateful to Shri Kulkarni, Daniel Reichart, James Rhoads, and Phil Solomon for useful discussions. TJG is supported by the Sherman Fairchild Foundation.

REFERENCES

- Barger, A. J., Cowie, L. L., & Sanders, D. B. 1999, *ApJ* 518, L5
 Bloom, J. S., Djorgovski, S. G., Kulkarni, S. R., & Frail, D. A. 1998, *ApJ* 507, L25
 Bloom, J. S., et al. 1999a, *Nature* 401, 453
 Bloom, J. S., Sigurdsson, S., & Pols, O. R. 1999b, *MNRAS* 305, 763
 Bulik, T., Belczynski, K., & Zbijewski, W. 1999, *A&AS* 138, 483
 Costa, E., et al. 1997, *Nature* 387, 783
 Dickey, J. M. & Lockman, F. J. 1990, *ARA&A* 28, 215
 Djorgovski, S. G., Kulkarni, S. R., Bloom, J. S., & Frail, D. A. 1999, *GCN* 289
 Djorgovski, S. G., Kulkarni, S. R., Bloom, J. S., Goodrich, R., Frail, D. A., Piro, L., & Palazzi, E. 1998, *ApJ* 508, L17
 Djorgovski, S. G., et al., in preparation
 Draine, B. T. 2000, *ApJ* 532, 273
 Eichler, D., Livio, M., Piran, T., & Schramm, D. N. 1989, *Nature* 340, 126
 Esin, A. A. & Blandford, R. D. 2000, *ApJ Lett*, in press, (astro-ph/0003415)
 Frail, D. A., Kulkarni, S. R., Nicastro, L., Feroci, M., & Taylor, G. B. 1997, *Nature* 389, 261
 Fruchter, A., priv. comm.
 Fruchter, A., Krolik, J., & Rhoads, J. 2000, *ApJ* submitted
 Galama, T., et al. 1999, *Nature* 398, 394
 Galama, T., et al. 2000, *ApJ* 536, 185
 Galama, T. J., et al. 1998a, *ApJ* 497, L13
 Galama, T. J., et al. 1998b, *Nature* 395, 670
 Galama, T. J., Wijers, R. A. M. J., Bremer, M., Groot, P. J., Strom, R. G., Kouveliotou, C., & van Paradijs, J. 1998c, *ApJ* 500, L97
 Groot, P. J., et al. 1998, *ApJ* 493, L27
 Halpern, J. P., Kemp, J., Piran, T., & Bershad, M. A. 1999, *ApJ* 517, L105
 Halpern, J. P., Thorstensen, J. R., Helfand, D. J., & Costa, E. 1998, *Nature* 393, 41
 Harrison, F. A., et al. 1999, *ApJ* 523, L121
 Heise, J., et al. 1999, *IAUC* 7099
 in 't Zand, J. J. M., et al. 1998, *ApJ* 505, L119
 Kommers, J. M., Lewin, W. H. G., Kouveliotou, C., van Paradijs, J., Pendleton, G. N., Meegan, C. A., & Fishman, G. J. 2000, *ApJ* 533, 696
 Kulkarni, S. R., et al. 1998, *Nature* 393, 35
 Kuulkers, E., et al. 2000, *ApJ*, in press (astro-ph/0003258)
 Madau, P., Pozzetti, L., & Dickinson, M. 1998, *ApJ* 498, 106
 Metzger, M. R., et al. 1997, *Nature* 387, 879
 Mochkovitch, R., Hernanz, M., Isern, J., & Martin, X. 1993, *Nature* 361, 236
 Morrison, R. & McCammon, D. 1983, *ApJ* 270, 119
 Owens, A., et al. 1998, *A&A* 339, L37
 Paczyński, B. 1998, *ApJ* 494, L45
 Piro, L. 2000, in *X-Ray Astronomy '99: Stellar Endpoints, AGN and the Diffuse X-ray Background* (:), in press (astro-ph/0001436)
 Predehl, P. & Schmitt, J. H. M. M. 1995, *A&A* 293, 889
 Ramaprakash, A. N., et al. 1998, *Nature* 393, 43
 Reichart, D. E. 1999, *ApJ* 521, L111
 Reichart, D. E., et al. 1999, *ApJ* 517, 692
 Rhoads, J. E. 1997, *ApJ* 487, L1
 Sanders, D. B. & Mirabel, I. F. 1996, *ARA&A* 34, 749
 Solomon, P. M. & Edmunds, M. G. (eds.) 1980, (Oxford:Pergamon)
 Solomon, P. M., Rivolo, A. R., Barrett, J., & Yahil, A. 1987, *ApJ* 319, 730
 Stanek, K. Z., Garnavich, P. M., Kaluzny, J., Pych, W., & Thompson, I. 1999, *ApJ* 522, L39
 Totani, T. 1997, *ApJ* 486, L71
 van Paradijs, J., et al. 1997, *Nature* 386, 686
 van Paradijs, J., Kouveliotou, C., & Wijers, R. A. M. J. 2000, *ARA&A* 38, in press
 Vreeswijk, P., et al. 1999a, *GCN* 324
 Vreeswijk, P. M., et al. 2000, in press (astro-ph/0009025) *ApJ*
 Vreeswijk, P. M., et al. 1999b, *ApJ* 523, 171
 Waxman, E. & Draine, B. T. 2000, *ApJ* 537, 796
 Wijers, R. A. M. J., Bloom, J. S., Bagla, J. S., & Natarajan, P. 1998, *MNRAS* 294, L13
 Wijers, R. A. M. J. & Galama, T. J. 1999, *ApJ* 523, 177
 Woosley, S. E. 1993, *ApJ* 405, 273

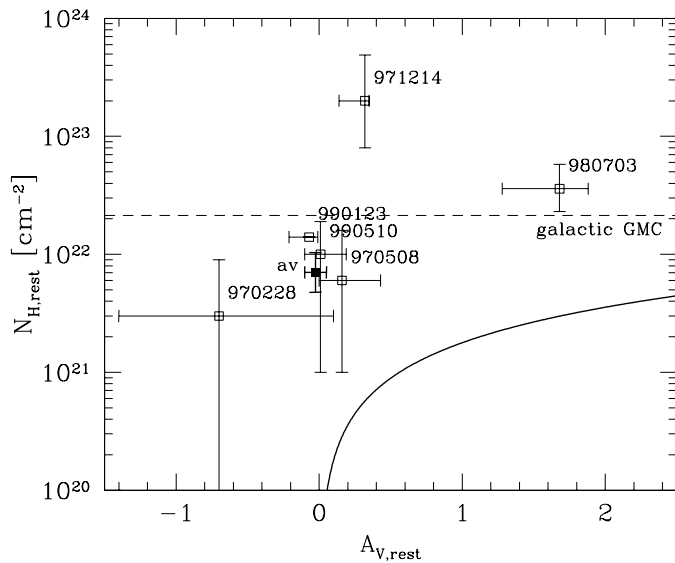


FIG. 1.— The hydrogen column density N_{H} versus the optical extinction at V band $A_{V,r}$ for a number of γ -ray burst afterglows; data are from table 1. The solid curve is the Galactic A_V - N_{H} relation (Predehl & Schmitt 1995). The solid symbol is the weighted mean of the four lowest points, assuming 50% for the unknown error of N_{H} for GRB 990123. The dashed line shows the average column density of a giant molecular cloud of $170M_{\odot}/\text{pc}^2$ (Solomon et al. 1987).

TABLE 1

The results of fitting a single power law plus dust absorption (eq. 1) and the results of fitting a broken power law plus dust absorption (eq. 2) to the X-ray to optical/infrared spectral flux distributions at the given epoch of γ -ray burst afterglows (see text for fits and parameter and sample definitions). ν_c and A_V are in the rest frame if z is known. References and notes: β_X and N_H are from Owens et al. (1998), unless stated otherwise; 970228 (Galama et al. 2000, Djorgovski et al. 1999); 970508 (Galama et al. 1998a, Galama et al. 1998c, Bloom et al. 1998); 971214 (Ramaprakash et al. 1998, Halpern et al. 1998, Wijers & Galama 1999, Kulkarni et al. 1998; in the fit we excluded the infrared data because of the observed spectral bump Ramaprakash et al. 1998); 980329 (Reichart et al. 1999, in 't Zand et al. 1998); 980519 (Halpern et al. 1999); 980703 (Vreeswijk et al. 1999b [β_X , N_H], Djorgovski et al. 1998); 990123 (Piro 2000 [Fig. 6, β_X], Galama et al. 1999, Heise et al. 1999 [N_H]); 990510 (Harrison et al. 1999, Stanek et al. 1999, Kuulkers et al. 2000, Vreeswijk et al. 1999a).

GRB	Epoch (UT)	single power law plus dust				broken power law plus dust					β_X	N_H ($\times 10^{21}$)	z
		$\log(F_{V0})$ (Jansky)	β	A_{Vr}	χ^2/dof	$\log(F_{V0})$ (Jansky)	β	A_{Vr}	$\log \nu_c$	χ^2/dof			
970228	0228.99	$-5.2^{+0.4}_{-0.5}$	$0.63^{+0.13}_{-0.13}$	$-0.8^{+0.7}_{-0.7}$	0.3/1	$-5.1^{+0.5}_{-0.6}$	$0.46^{+0.29}_{-0.14}$	$-0.7^{+0.7}_{-0.8}$		0.3/1	$0.96^{+0.19}_{-0.19}$	3^{+6}_{-4}	0.695
970508	0510.98	$-4.50^{+0.12}_{-0.11}$	$0.84^{+0.06}_{-0.05}$	$0.02^{+0.15}_{-0.14}$	2.2/3	$-4.38^{+0.14}_{-0.10}$	$0.50^{+0.35}_{-0.20}$	$0.16^{+0.16}_{-0.27}$		2.1/3	$0.99^{+0.29}_{-0.07}$	6^{+10}_{-5}	0.835
971214	1215.50	$-4.72^{+0.14}_{-0.13}$	$0.90^{+0.05}_{-0.05}$	$0.38^{+0.11}_{-0.09}$	0.2/1	$-4.81^{+0.40}_{-0.08}$	$0.38^{+0.60}_{-0.03}$	$0.32^{+0.18}_{-0.03}$		1.8/1	$1.03^{+0.51}_{-0.22}$	200^{+290}_{-120}	3.42
980703	0704.40	$-4.09^{+0.07}_{-0.06}$	$1.05^{+0.03}_{-0.03}$	$1.63^{+0.20}_{-0.20}$	2.0/1	$-4.06^{+0.23}_{-0.07}$	$1.01^{+0.06}_{-0.25}$	$1.68^{+0.40}_{-0.20}$		2.1/1	18^{+2}_{-3}	36^{+22}_{-13}	0.966
990123	0124.65	$-4.94^{+0.06}_{-0.06}$	$0.66^{+0.03}_{-0.03}$	$-0.20^{+0.17}_{-0.16}$	2.0/5	$-4.93^{+0.22}_{-0.06}$	$0.65^{+0.04}_{-0.15}$	$-0.07^{+0.14}_{-0.06}$	$18.8^{+0.6}_{-3.4}$	1.9/5	$0.97^{+0.04}_{-0.04}$	14	1.60
990510	0511.26	$-4.20^{+0.08}_{-0.09}$	$0.86^{+0.04}_{-0.04}$	$-0.22^{+0.23}_{-0.23}$	0.15/2	$-4.09^{+0.11}_{-0.18}$	$0.60^{+0.25}_{-0.20}$	$0.01^{+0.11}_{-0.18}$	$16.7^{+3.2}_{-1.7}$	0.0/3	$1.12^{+0.12}_{-0.12}$	10^{+9}_{-9}	1.62
980329	0402.99	$-5.70^{+0.17}_{-0.20}$	$0.91^{+0.10}_{-0.07}$	$2.9^{+1.1}_{-0.8}$	0.0/0	$-5.65^{+0.30}_{-0.22}$	$0.85^{+0.15}_{-0.20}$	$3.0^{+1.3}_{-0.9}$		0.4/0	$1.63^{+0.41}_{-0.36}$	10^{+8}_{-4}	
980519	0520.34	$-4.34^{+0.16}_{-0.15}$	$0.98^{+0.06}_{-0.06}$	$0.8^{+0.4}_{-0.4}$	0.2/2	$-4.31^{+0.26}_{-0.17}$	$0.92^{+0.11}_{-0.27}$	$0.9^{+0.6}_{-0.4}$		0.4/2	$1.52^{+0.70}_{-0.57}$	4^{+10}_{-5}	